Cavendish-HEP-98/13
RAL-TR-1998-063
September 1998

The phenomenology of $W^{\pm}H^{\mp}$ production at the Large Hadron Collider

Stefano Moretti[a] and Kosuke Odagiri[b]

a) Rutherford Appleton Laboratory, Chilton, Didcot, Oxon OX11 0QX, UK.

b) Cavendish Laboratory, University of Cambridge, Madingley Road, Cambridge CB3 0HE, UK.

Abstract

Barrientos Bendezú and Kniehl [1] recently suggested that $W^{\pm}H^{\mp}$ associated production may be a useful channel in the search for the elusive heavy charged Higgs bosons of the 2 Higgs Doublet Model at the Large Hadron Collider. We investigate the phenomenology of this mechanism in the Minimal Supersymmetric Standard Model, with special attention paid to the most likely heavy Higgs decay, $H^{\mp} \to tb \to b\bar{b}W^{\mp}$, and to the irreducible background from top pair production. We find that the semi-leptonic signature '$b\bar{b}W^{+}W^{-} \to b\bar{b}\ jj\ \ell\ +$ missing momentum' is dominated by top-antitop events, which overwhelm the charged Higgs signal over the heavy mass range that can be probed at the CERN collider.

PACS numbers: 12.60.Fr, 12.60.Jv, 13.85.-t, 14.80.Cp.

Electronic mails: moretti@v2.rl.ac.uk, odagiri@hep.phy.cam.ac.uk.

1. Introduction

In Ref. [1], Barrientos Bendezú and Kniehl pointed out that the processes

$$b\bar{b} \to W^{\pm}H^{\mp} \tag{1}$$

and

$$gg \to W^{\pm}H^{\mp} \tag{2}$$

can be used in the search for the heavy ($M_{H^\pm} > m_t + m_b$) charged Higgs bosons $H^\pm$ of the 2 Higgs Doublet Model (2HDM) at the Large Hadron Collider (LHC).

This result is particularly welcome, since it has been remarked in several occasions (see Ref. [2] for an overview) that at present it is not at all certain that such particles can be detected at the LHC, even in the Minimal Supersymmetric Standard Model (MSSM), if the typical energy scale of Supersymmetry (SUSY) is much greater than the charged Higgs mass.

Previous studies have shown that, if $M_{H^\pm} > m_t + m_b$, the chances of $H^\pm$ detection at the LHC are reliant only on two production mechanisms: the subprocesses $bg \to tH^\pm$ [3] and $bq \to bq'H^\pm$ [4] and provided that $M_{H^\pm} \lesssim 300 - 400$ GeV [5]. These channels generally have poor signal-to-background ratios, as the event signatures always involve a large number of jets, which is the typical noise of a hadron-hadron machine.

When $H^\pm$'s are heavy, for $M_{\rm SUSY} \gg M_{H^\pm}$, they decay almost exclusively to $\bar{b}t(b\bar{t})$ [6]. In addition, hadronic signatures of $W^\pm$ bosons produced in top decays are normally selected in order to allow for the $H^\pm$ mass reconstruction. Therefore, at first sight, it appears that the signals (1)–(2) advocated in Ref. [1] as a useful source of Higgs events may be swamped by the irreducible background from top pair production,

$$q\bar{q} \to t\bar{t} \qquad \text{and} \qquad gg \to t\bar{t}, \tag{3}$$

with subsequent decay through the intermediate state[1] $b\bar{b}W^+W^-$. In order to understand whether this is the case, we made a detailed signal-to-background analysis and found that top-antitop production and decay indeed overwhelms the new Higgs signal.

The plan of this paper is as follows. In the next Section we describe the details of the calculation and list the parameter values adopted. Section 3 is devoted to the discussion of results. We present our conclusions in Section 4.

2. Calculation

We generated the signal cross sections by using the formulae of Ref. [1]. However, for phenomenological analyses we need to supplement those expressions in several ways.

Firstly, their matrix elements (MEs) do not include the $W^\pm$ boson decay and thus carry no information on the angular distributions of the fermion pair it produces. For the $H^\pm$ this does not matter, since scalar particles decay isotropically. However, even

[1] Alternatively, in a narrow window in $M_{H^\pm}$ and only at low $\tan\beta$, the charged Higgs bosons can decay to $W^\pm h$ pairs, where h represents the lightest Higgs boson. Although we will not treat this case here, we note that even in this channel the final state is identical to that of top-antitop, as $h \to b\bar{b}$ is dominant over most of the SUSY parameter space.

in this case one has to provide the correct kinematics for the decay sequence $H^\pm \to tb \to b\bar{b}W^\pm \to b\bar{b}jj$ (where j represents a light quark jet produced in the $W^\pm$ decay), which we have done by computing the exact ME constructed by means of the `HELAS` subroutines [7]. As for the $W^\pm$ decay in the production channels (1) and (2), we have re-evaluated their MEs with the additional insertion of the $W^\pm$ boson decay currents. For the $b\bar{b}$ fusion case, the actual expression is the same as for the $bq \to bq'H^\pm$ process calculated in [4] and recently modified in [8], but with some leg crossings. For the gg fusion case, the result is simply the replacement

$$\lambda(s, M^2_{W^\pm}, M^2_{H^\pm}) \to 4g^2 M^2_{W^\pm}|\mathcal{G}_{W^\pm}|^2[2(p_1 \cdot p_{H^\pm})(p_2 \cdot p_{H^\pm}) - (p_1 \cdot p_2)M^2_{H^\pm}] \quad (4)$$

in equation (8) of [1], where $g^2 = 4\pi\alpha_{em}/\sin\theta^2_W$, $|\mathcal{G}_{W^\pm}|^2 = [(p^2_{W^\pm} - M^2_{W^\pm})^2 + (\Gamma_{W^\pm}M_{W^\pm})^2]^{-1}$, with $p_{H^\pm}$, $p_{W^\pm}$, p_1 and p_2 the four-momentum of the $H^\pm$, $W^\pm$, first and second lepton, say ℓ and ν_ℓ, from the gauge boson decay, respectively.

Secondly, their MEs for the gg fusion processes do not involve squark loops, this preventing one from studying possible effects of the SUSY partners of ordinary quarks, when their mass is below the TeV scale. For example, these corrections are expected to be sizable in the MSSM, which is adopted here as the default SUSY framework. In this respect, we have modified the gg triangle formula of Ref. [1] for the case of intermediate neutral Higgs production (top graph in Fig. 2 there), by inserting the well known [5, 9, 10] squark loop terms [5].

Conversely, we have not included here the contribution of the box diagrams (bottom two graphs of Fig. 2 in Ref. [1]), for which the authors of that paper found no compact expression. According to their curves in Fig. 5 [1], this should result in an overestimate of the total cross section of subprocess (2), as the triangle and box diagrams interfere destructively. The overall effect is however negligible at large $\tan\beta$, the regime where the $W^\pm H^\mp$ cross section is larger (whereas, for $\tan\beta = 1.5$, it can at times be more than a factor of two: see Fig. 3 of Ref. [1]). In addition, this is particularly true for $M_{H^\pm} \gg m_t$, the mass interval with which this paper is concerned. Indeed, in most of our plots we will concentrate on that portion of the MSSM parameter space, for which we expect our results to be reliable.

Finally, all our calculations for the signal were tested against the original cross sections of [1], and also using MadGraph [11] for the case $b\bar{b} \to W^\pm H^\mp$.

For the background we have assumed that the QCD contribution is reducible by cuts on the reconstructed top and $W^\pm$ masses. Therefore, we studied the top pair background only, which is anyhow the dominant component of the final state $b\bar{b}U\bar{D}\ell\bar{\nu}_\ell$ where U and D refer to up- and down-type massless quarks and $\ell = e$ or μ. We have considered both $q\bar{q} \to t\bar{t} \to b\bar{b}U\bar{D}\ell\bar{\nu}_\ell$ and $gg \to t\bar{t} \to b\bar{b}U\bar{D}\ell\bar{\nu}_\ell$, which we generated at leading order using the HELAS library [7]. The outputs of the corresponding code agree with the results given in Ref. [12] when the $W^\pm$'s are on the mass shell. In fact, notice that finite widths effects of top quarks, gauge and charged Higgs bosons have been taken into account here.

Concerning the values of the various MSSM parameters entering the computation of the signal processes (1)–(2) (and, marginally, the MSSM top width), we proceeded as follows. First, we produced the masses and the widths of the Higgs bosons by means of the two loop relations of Ref. [13] (see also [14]). To simplify the discussion, we have assumed a universal soft Supersymmetry–breaking mass $m^2_{\tilde{u}} = m^2_{\tilde{d}} \equiv m^2_{\tilde{q}}$, and negligible mixing in the stop and sbottom mass matrices, $A_t = A_b = \mu = 0$. Second, the MSSM Higgs widths were generated using the program `HDECAY` [15], which in turn uses mass relations at the same perturbative level. Squark masses entering the loops in the gg induced signal processes have been kept as independent parameters and their values varied between 300 GeV and 1 TeV, the minimum figure being chosen in such a way that the superpartners do not enter the $H^\pm$ decay chain, as for the upper mass of the latter we have taken the value of 600 GeV. Further notice that squark masses have been considered degenerate, for illustrative purposes, so that only sbottom and stop loops in practice contribute.

In the numerical calculations presented in the next Section we have adopted the following values for the electromagnetic coupling constant and the weak mixing angle: $\alpha_{em} = 1/128$ and $\sin^2\theta_W = 0.2320$. The strong coupling constant α_s, which appears in higher orders in the computation of the charged Higgs decay widths and enters in some of the production mechanisms, has been evaluated at one or two loops, depending on the Parton Distributions Functions (PDFs) used, with $\Lambda^{(4)}_{\overline{\mathrm{MS}}}$ (for the number of active flavours $N_f = 4$) input according to the values adopted in the fits of the latter. For the leading-order (LO) package CTEQ4L [16], which constitutes our default set (as in [1]), we have taken 236 MeV. The factorisation/renormalisation scale Q entering in both α_s and the PDFs was set to $\sqrt{\hat{s}}$, the centre-of-mass (CM) energy at the partonic level, in all processes generated.

In order to have an estimate of the dependence of the bottom quark and gluon structure function we tested our signal rates against the next-to-leading (NLO) sets MRS(R1,R2,R3,R4) [17], i.e., the Martin-Roberts-Stirling packages of the same 'generation' as the CTEQ ones considered here, plus the newly presented sets MRST [18], which embody new data and an improved description of the gluons at small x, along with a dedicated treatment of the heavy quark structure functions. Typical differences were found to be within 15–20%, at cross section level, with the shape of the relevant differential distributions being little affected by the treatment of the partons inside the proton.

For the gauge boson masses and widths we have taken $M_Z = 91.1888$ GeV, $\Gamma_Z = 2.5$ GeV, $M_{W^\pm} = 80.23$ GeV and $\Gamma_{W^\pm} = 2.08$ GeV. For the top mass we have used $m_t = 175$ GeV with the corresponding width evaluated at tree-level in the MSSM (yielding $\Gamma_t = 1.55$ GeV if $M_{H^\pm} > m_t - m_b$, the Standard Model value). Bottom quarks have been considered massless when treated as partons inside the proton, while a finite value of 4.25 GeV (pole mass) has been retained in the final states. Note that in calculating the ME for the decay process $H^\pm \to tb$ the Yukawa mass of the b quark has been run up to the charged Higgs mass scale, in accordance to the way the corresponding width has been computed. Finally, for simplicity, we set the Cabibbo-Kobayashi-Maskawa matrix element V^{bt}_{CKM} to one.

3. Results

As it is impractical to cover all possible regions of the MSSM parameter space $(M_A, \tan\beta)$, we concentrate here on the two representative (and extreme) values $\tan\beta = 1.5$ and 30, and on masses of the charged Higgs boson in the range 160 GeV

$\lesssim M_{H^\pm} \lesssim 600$ GeV. The large bibliography existing on the MSSM Higgs decay phenomenology should allow one to easily extrapolate our results to other values of $\tan\beta$ [5].

We consider the semi-leptonic event modes for processes (1)–(3):

$$W^\pm H^\mp \to W^\pm tb \to b\bar{b}W^+W^- \to b\bar{b}\ \ jj\ \ \ell + \text{missing energy/momentum}. \qquad (5)$$

In fact, we base our signal selection procedure on the following general requirements.

1. High purity double b quark tagging. This may be expected to yield an efficiency of at least 50% per fiducial b jet [19, 20]. This is essential considering the large rate of $W^\pm +$ jet events with light quarks and gluons. All our results will assume 100% bottom quark tagging efficiency ϵ_b, and thus will eventually need to be multiplied by the actual ϵ_b^2 once we will have the LHC detectors running.

2. Lepton isolation at high transverse momentum. Selecting semi-leptonic events should enable one to use the high p_T and isolated lepton (electron and/or muon) originating from the $W^\mp$ produced in association with the $H^\mp$ as a clean trigger[2] [1]. In addition, the light quark jets j coming from the secondary $W^\mp$, from $H^\mp \to tb \to b\bar{b}W^\mp$, would allow for the reconstruction of the Higgs mass peak. However, one should recall that the two gauge bosons could decay the other way round, this in principle spoiling the efficiency of the signal selection. In practice, one can remove the contribution from semi-leptonic Higgs decays by simply imposing cuts on the reconstructed top mass.

3. $W^\pm$ and t mass reconstruction in two and three jet combinations, respectively, to eliminate QCD multi-jet production.

Our results are shown throughout Figs. 1–8. When differential spectra are plotted, the three representative parameter space points of $M_A = 200$, 400 and 600 GeV at $\tan\beta = 30$ have been chosen, corresponding to $M_{H^\pm} = 214$, 407 and 605 GeV, respectively.

As a preliminary exercise, in order to understand the kinematics of the signal and background better, and possibly to pin down systematic differences which can be used in the selection of candidate Higgs events, we compare their total and differential rates in the channel (5) without the usual detector cuts on transverse momenta and pseudorapidity. In fact, both processes have finite production rates at lowest order over all of the phase space.

The main frame of Fig. 1 shows the signal (with no squark loop contributions) and background cross sections before any detector or selection cuts, evaluated at the LHC energy (14 TeV) and plotted against the $H^\pm$ mass for the two values of $\tan\beta$. The background remains constant as a function of the charged Higgs mass, except when the decay $t \to bH^+$ is kinematically allowed. It is found that even when the signal cross section is the highest the signal/background ratio is less than one in a thousand. Notice that at decay level, see eq. (5), the signal rates suffer from a further small depletion (in addition to that due to finite width effects) as compared to the on-shell ones of

[2]For the time being, we neglect $W^\pm \to \tau\nu_\tau$ decays, which should also be identified easily thanks to their 'one-prong' signatures, as remarked in [1].

Ref. [1], if the latter are multiplied by the relevant branching ratios (BRs). This is due to the fact that the Goldstone part of the longitudinal component of the $W^\pm$ boson (i.e., the wave-function term proportional to $p^\mu_{W^\pm}/M_{W^\pm}$) produced in association with the $H^\mp$ scalar in $b\bar{b}$ fusion (included in that reference) does not survive the decay into 'massless' fermions. The effect depends on $\tan\beta$, owning the structure of the MSSM couplings in the $\Phi W^\pm H^\mp$ vertices, where $\Phi = H$ and h, and on the relative strength of the two contributing diagrams (see Figs. 1–2 of Ref. [1]).

In the central insert of Fig. 1 we study possible virtual effects of SUSY, manifesting itself in the triangle diagrams of gg fusion. In fact, we plot the ratio of the signal cross sections obtained by adding the rates of both suprocesses (1) and (2), the latter including squark loops, against those calculated when such contributions are neglected. As already remarked in the literature [10], sizable SUSY effects in the gg subprocess are expected only for squark masses below 500 GeV or so and particularly at small $\tan\beta$. Thus, in our plot we present the ratios for $m_{\tilde{q}} = 300$ and 500 GeV at $\tan\beta = 1.5$ only. Given the remarks made in the Introduction, concerning our remotion of the box diagrams and, consequently, of the cancellations against the triangle ones (which we would further think to be active for virtual squark contributions as well), our numbers should in this circumstance be intended as a sort of *upper limit* that one might expect from such SUSY effects. From this prospect, it is then clear that production rates can increase by no more than 20% or so, and provided squark masses are rather low, a correction indeed comparable to the combined uncertainties related to the b quark and gluon PDFs in (1) and (2), respectively, and to the scale dependence of the gg production rates [10]. For this reasons, and to simplify the discussion as well, hereafter, we will neglect altogether the squark loop contributions in our signal rates.

The differential spectra are displayed in Figs. 2–6. In particular, we plot[3]

- the lepton, light quark, b jet and missing transverse momentum;
- the lepton, light quark and b jet pseudorapidity;
- the lepton/light quark jet and lepton/b jet separation, defined by the variable $\Delta R = \sqrt{(\Delta\eta)^2 + (\Delta\phi)^2}$ in terms of pseudorapidity η and azimuth ϕ.

Furthermore, we present the invariant mass spectra of the following systems:

- bb, as obtained by pairing the two jets with displaced vertices;
- three jets, with only one b jet involved;
- four jets, involving all four jets in the final state.

The combinatorics in the three, four and lepton/light quark jet systems is accounted for by simply plotting all possible momentum combinations each with the same event weight. In other terms, the signal spectra contain both hadronic and leptonic $W^\pm/H^\mp$ decay modes (but not their interference, that we expect negligible), which have in fact different kinematics. The two component will eventually be separated by imposing

[3]We make no distinction between b and $\bar{b}$ jets, tacitly assuming neither jet charge determination nor lepton tag.

cuts around the reconstructed top quark mass, as mentioned before. In contrast, the background spectra, obviously, do not depend on whether the top or the antitop decays leptonically.

The usual distributions in p_T and η indicate the effects of detector acceptance cuts on the signal and background samples. Neither of these affects the event rates significantly. The distribution in ΔR indicates that the requirement of lepton/jet separation will not harm the event rates either. Furthermore, the signal and background distributions are very similar and it is clear that none of these variables can profitably be used to optimise the selection procedure. Incidentally, we mention that we also had a look at the transverse momentum and pseudorapidity of the three hadronic systems introduced above, without finding any significant difference between Higgs and top events.

Presumably, the invariant mass distributions, see Fig. 5 and 6 for the purely hadronic and semi-leptonic systems, respectively, will give us the greatest chance of removing the background. By imposing cuts on the two light quark jet and two light quark plus bottom jet invariant masses around the $W^\pm$ and top quark resonances, respectively, we can remove most of the QCD noise, having to deal finally with the semi-leptonic top pair decays which is the greatest challenge. As a matter of fact, di-jet pairs of light quarks from $t\bar{t}$ events naturally peak at $M_{W^\pm}$, exactly as those from $W^\pm H^\mp$ do. As for the three jet systems, mispairings of b quarks with the wrong $W^\pm$ have more severe effects on the signal than on the background, as one can intuitively expect from the production dynamics and as it can be appreciated in the middle plot of Fig. 5 (note the height of the peak for $t\bar{t}$ events, as compared to that of the $W^\pm H^\mp$ ones).

Here we propose the following related and complementary cuts on invariant masses. For a start, we put ourselves in the favourable phenomenological position that the charged Higgs mass $M_{H^\pm}$ is known, e.g., thanks to a previous detection of the light scalar Higgs h and to the measurement of its couplings. Under these circumstances, in order to enhance the $W^\pm H^\mp$ to $t\bar{t}$ rates, one can impose a cut on the invariant mass of the bb pair. Since in the signal both bottom jets originate from the $H^\pm$ scalar and assuming that $H^\pm \to b\bar{b}W^\pm$, the invariant mass squared M_{bb} must be below $\sqrt{M_{H^\pm}^2 - M_{W^\pm}^2}$ (apart from finite width effects). The distribution from top pair events has a characteristic scale of $2m_t$ and therefore, at low $M_{H^\pm}$, it can be filtered out by setting a sufficiently low cut. The gain for the signal-to-background rate is large if $H^\pm$ is reasonably ($m_t < M_{H^\pm} < 2m_t$) light (solid and dashed curves in Fig. 5, upper plot), whereas for heavy charged Higgs bosons, when $M_{H^\pm}$ is of the order $2m_t$ or greater, the cut is not useful (dotted curve in Fig. 5, upper plot). However, one should note that this selection cut can be utilised successfully only when $M_{H^\pm}$ is approximately known, and is of limited use even then, since it only removes the background from regions of phase space far away from reconstructing the charged Higgs mass peak.

Similarly, one can impose a cut on the invariant mass of a $b\ell$ pair, where b is the bottom jet which does not reproduce the top quark with the light di-jet pair (i.e., the one yielding the reconstructed m_t further away from its actual value). Here, the selection works because for the $t\bar{t}$ background, if both top and $W^\pm$ are on the mass shell, one has $M_{b\ell} < \sqrt{m_t^2 - M_{W^\pm}^2}$. However, it should be noticed that the Higgs production mechanism can really push the $M_{b\ell}$ value beyond $\sqrt{m_t^2 - M_{W^\pm}^2}$ only if $M_{H^\pm}$ is large enough: see dashed and dotted curves in Fig. 6, for $M_{b\ell/j} \gtrsim 160$ GeV. Failing this condition, the suppression against the signal itself can be quite large (e.g., an additional rejection factor of five for $M_{H^\pm} = 214$ GeV at $\tan\beta = 30$). However, it turns out that such a constraint is definitely necessary to bring down the background rates to manageable levels (as it contributes with an additional factor of thirty or so to the suppression of top-antitop events), so that we employ it even at low $M_{H^\pm}$ values.

In addition, we have made the following, more standard cuts:

1. isolation of the two bottom jets from the light quark jets and from each other, as we tentatively set the azimuthal-pseudorapidity separation at $\Delta R_{bb,bj} > 0.7$ between them[4];

2. for an isolated lepton, we impose the cut $\Delta R_{\ell b,\ell j} > 0.4$ between the lepton and all jets;

3. the light quark jet pair mass M_{jj} within $M_{W^\pm} \pm 10$ GeV;

4. the light quark jet pair and a bottom quark jet combine at least once to a mass M_{bjj} of $m_t \pm 10$ GeV;

5. all one-particle pseudorapidities (of leptons, light and heavy quarks) are constrained within a detector region of 2.5;

6. the transverse momentum cut was set at 20 GeV for all jets and leptons, and for the missing transverse momentum as well.

Fig. 7 displays the total rates for signal and background after the above selection cuts have been enforced. Since the latter depends on the value of $M_{H^\pm}$, the cross section for events of the type (3) is no longer constant when $M_{H^\pm} \gtrsim m_t$. However, given the weak dependence of $M_{H^\pm}$ on $\tan\beta$, the two top-antitop curves overlap in that mass range. Although the signal-to-background ratio has greatly improved, as compared to the initial situation in Fig. 1, for any combination of $M_{H^\pm}$ and $\tan\beta$, this is still very small, at least one part in a hundred, so to presumably dash away any hopes of resolving the Higgs peak.

In fact, to be realistic, one should expect a four jet mass resolution of no less than 10 GeV, given the usual uncertainties in reconstructing parton directions and energies from multi-hadronic events. Therefore, in Fig. 8, we have binned the invariant masses of the $bbjj$ system in signal and background using that value. If one does so, it is clear that the Higgs mass peaks at 214, 407 and 605 GeV (with Breit-Wigner width $\Gamma_{H^\pm}$ of 1.2, 4.4 and 6.1 GeV, respectively), at $\tan\beta = 30$, are overwhelmed by the top-antitop events. Seemingly, even where the signal is more pronounced over the background (at large $M_{H^\pm}$), the excess amounts to no more than 10% at the most in the central bin. This is probably too little, further considering, on the one hand, the aforementioned uncertainties (PDFs, K-factors, etc.) and, on the other hand, that the event rate is poor, only around 1 fb prior to the vertex tagging efficiency ϵ_b^2 being applied. Needless to say, if one looks back at Fig. 7, similar conclusions should be expected for all other combinations of M_A and $\tan\beta$ considered here, finally recalling our systematic overestimate of the signal rates for low values of the latter.

[4]Note that we allow for the light quark jets to be arbitrarily close.

4. Conclusions

We believe that in the $H^{\mp} \to tb \to b\bar{b}W^{\mp}$ channel, *heavy* charged Higgs scalars of the Minimal Supersymmetric Standard Model produced in association with $W^{\pm}$ gauge bosons cannot be resolved at the LHC, via semi-leptonic W^+W^- decays, for Higgs masses in the range between $2m_t$ and 600 GeV (those producible at observable rate), at neither low nor high $\tan\beta$, because of the presence of the irreducible background from top-antitop events. Furthermore, our results can safely be applied to a more general 2 Higgs Double Model too (where mass and coupling constraints in the Higgs sector can be relaxed), given the extremely poor significance of the $W^{\pm}H^{\mp}$ rates over the $t\bar{t}$ ones. As for other hadronic collider environments, the prospects of detection at the Tevatron (Run II) are even more reduced, given the lower machine luminosity and since the production cross section of the signal is there about three orders of magnitude smaller than at the CERN accelerator (for detectable Higgs masses below 300 GeV or so), while the background only decreases by about two orders.

We have reached these conclusions after performing a detailed signal-to-background analysis, based on matrix element calculations of elementary $2 \to 6$ suprocesses, convoluted with up-to-date parton distribution functions, and exploiting dedicated selection cuts, beyond the usual requirements in transverse momentum and pseudorapidity. Although we have confined ourselves to the the parton level only, wherein jets are identified with partons, we are however confident that hadronisation and detector effects will not modify our main results.

Nonetheless, we would like to conclude this paper with a positive note. Charged Higgs production in association with $W^{\pm}$'s, via $b\bar{b}$ and gg fusion at hadron colliders, represents a novel mechanism, whose decay phenomenology is largely unknown and that should be investigated further, considering that the detection of this particle is *not at all* certain at the next generation of hadronic machines, especially in the heavy mass range. In this respect, we would like to advocate, for example, the consideration of non-Standard Model decay channels, involving squarks, sleptons and gauginos, which was beyond the intention of this study.

Acknowledgements

SM is grateful to the UK PPARC and KO to Trinity College and the Committee of Vice-Chancellors and Principals of the Universities of the United Kingdom for financial support. SM also thanks David Miller and Mike Seymour for useful discussions.

References

[1] A.A. Barrientos Bendezú and B.A. Kniehl, *preprint* MPI/PhT/98-054, July 1998, `hep-ph/9807480`.

[2] S. Moretti and K. Odagiri, *Phys. Rev.* **D57** (1998) 5773.

[3] J.F. Gunion, H.E. Haber, F.E. Paige, W.-K. Tung and S.S.D. Willenbrock, *Nucl. Phys.* **B294** (1987) 621.

[4] S. Moretti and K. Odagiri, *Phys. Rev.* **D55** (1997) 5627.

[5] See, for example:
J.F. Gunion, H.E. Haber, G.L. Kane and S. Dawson, *"The Higgs Hunter Guide"* (Addison-Wesley, Reading MA, 1990) and references therein.

[6] S. Moretti and W.J. Stirling, *Phys. Lett.* **B347** (1995) 291; Erratum, *ibidem*, **B366** (1996) 451;
A. Djouadi, J. Kalinowski and P.M. Zerwas, *Z. Phys.* **C70** (1996) 435.

[7] H. Murayama, I. Watanabe and K. Hagiwara, HELAS: HELicity Amplitude Subroutines for Feynman Diagram Evaluations, *KEK Report* 91–11, January 1992.

[8] S. Moretti, M.H. Seymour, K. Odagiri and B.R. Webber, in preparation.

[9] H. Georgi, S.L. Glashow, M.E. Machacek and D.V. Nanopoulos, *Phys. Rev. Lett.* **40** (1978) 692.

[10] M. Spira, A. Djouadi, D. Graudenz and P.M. Zerwas, *Nucl. Phys.* **B453** (1995) 17.

[11] T. Stelzer and W.F. Long, *Comp. Phys. Comm.* **81** (1994) 357.

[12] A. Ballestrero, E. Maina and M. Pizzio, *Phys. Lett.* **B387** (1996) 411.

[13] J.R. Espinosa and M. Quiros, *Phys. Lett.* **B266** (1991) 389;
R. Hempfling and A. Hoang, *Phys. Lett.* **B331** (1994) 99;
M. Carena, J. Espinosa, M. Quiros and C.E.M. Wagner, *Phys. Lett.* **B355** (1995) 209;
M. Carena, M. Quiros and C.E.M. Wagner, *Nucl. Phys.* **B461** (1996) 407.

[14] S. Heinemeyer, W. Hollik and G. Weiglein, *preprint* KA-TP-2-1998, March 1998, `hep-ph/9803277`;
S. Heinemeyer, talk given at the *International Workshop on Quantum Effects in the Minimal Supersymmetric Standard Model*, Barcelona, Spain, 9-13 September 1997, *preprint* KA-TP-18-1997, September 1997, `hep-ph/9803294`.

[15] A. Djouadi, J. Kalinowski and M. Spira, *Comput. Phys. Commun.* **108** (1998) 56.

[16] H.L. Lai, J. Huston, S. Kuhlmann, F. Olness, J.F. Owens, D. Soper, W.K. Tung and H. Weerts, *Phys. Rev.* **D55** (1997) 1280.

[17] A.D. Martin, R.G. Roberts and W.J. Stirling, *Phys. Lett.* **B387** (1996) 419.

[18] A.D. Martin, R.G. Roberts, W.J. Stirling and R.S. Thorne, *Eur. Phys. J.* **C4** (1998) 463.

[19] ATLAS Technical Proposal, CERN/LHC/94-43 LHCC/P2 (December 1994).

[20] CMS Technical Proposal, CERN/LHC/94-43 LHCC/P1 (December 1994).

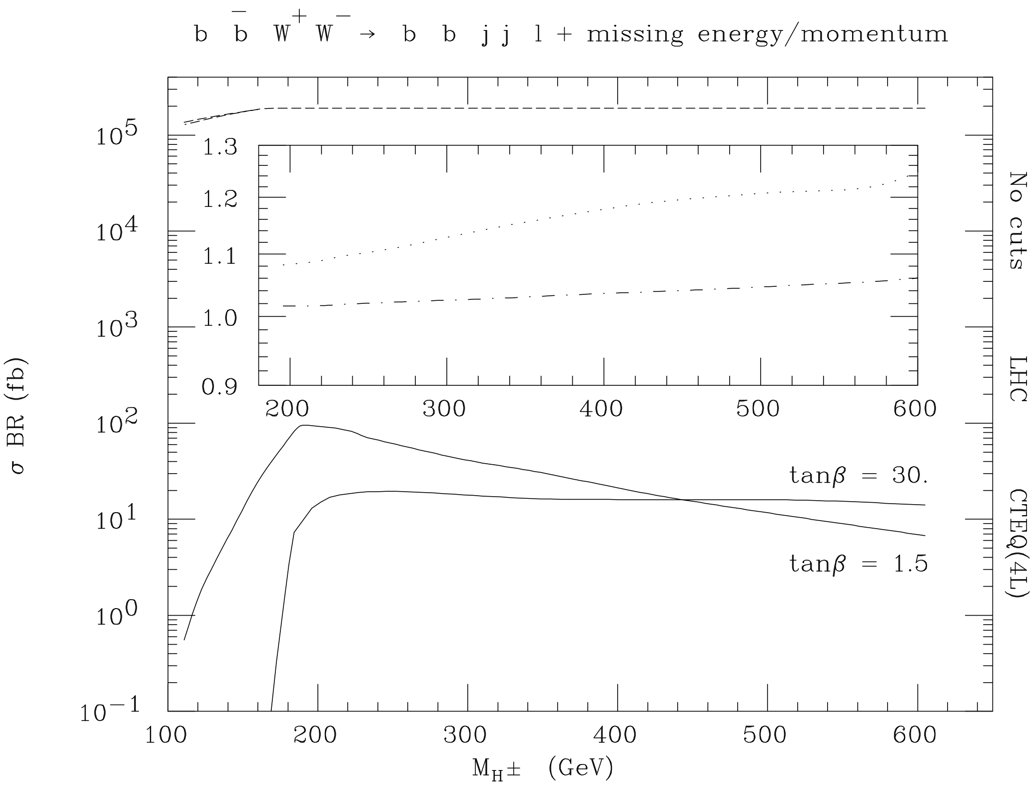

Figure 1: Total event rates for $W^\pm H^\mp$ (solid) and $t\bar{t}$ production (dashed) at the LHC, with no cuts implemented, using CTEQ(4L), as a function of $M_{H^\pm}$ for $\tan\beta = 1.5$ and $\tan\beta = 30$. In the blow up figure, the $W^\pm H^\mp$ production rates for $\tan\beta = 1.5$ including squark loop contributions, with $m_{\tilde{q}} = 300$ (dotted) and 500 (dot-dashed) GeV, divided by those obtained when the latter are neglected. For $\tan\beta = 30$, squark contributions are negligible, so that the same ratios would visually coincide with one.

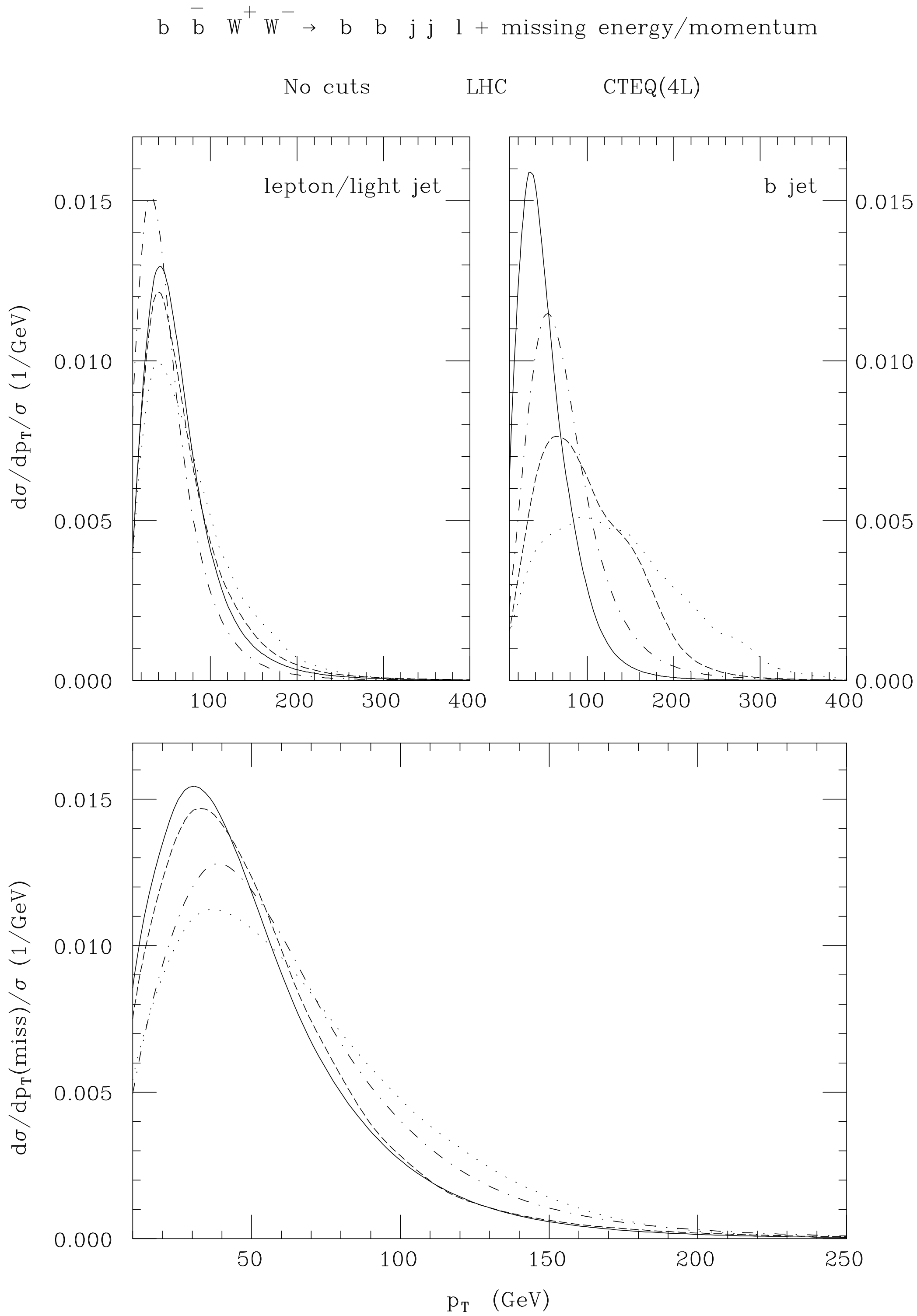

Figure 2: Differential spectra in lepton/light quark jet (top-left), b jet (top-right) and missing (bottom) transverse momentum. Here, $\tan\beta = 30$ and the $W^\pm H^\mp$ rates are plotted for $M_{H^\pm} = 214$ (solid), 407 (dashed) and 605 (dotted) GeV. As $M_{H^\pm} > m_t + m_b$, $t\bar{t}$ events have no MSSM parameter dependence (dot-dashed). No cuts have been implemented. The PDFs CTEQ(4L) have been used. Distributions are normalised to unity. Note that, in the case of the lepton and light quark jet, the curves coincide.

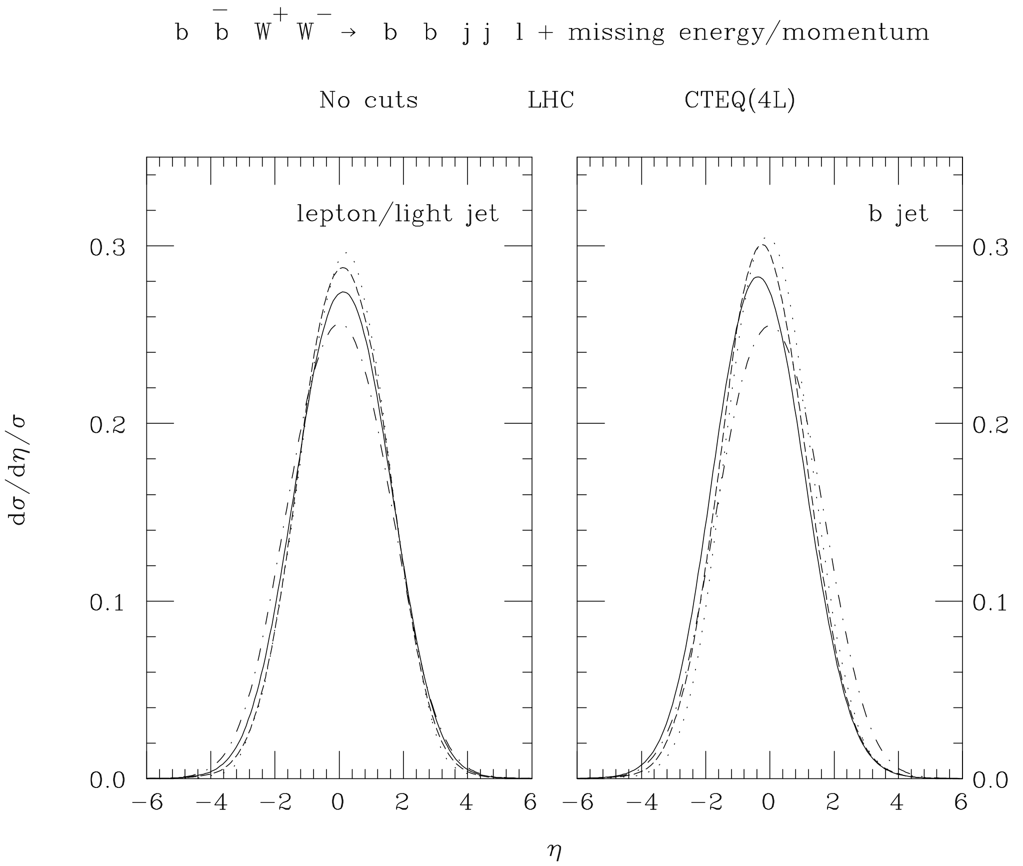

Figure 3: Differential spectra in lepton/light quark jet (left) and b jet (right) pseudorapidity. Here, $\tan\beta = 30$ and the $W^\pm H^\mp$ rates are plotted for $M_{H^\pm} = 214$ (solid), 407 (dashed) and 605 (dotted) GeV. As $M_{H^\pm} > m_t + m_b$, $t\bar{t}$ events have no MSSM parameter dependence (dot-dashed). No cuts have been implemented. The PDFs CTEQ(4L) have been used. Distributions are normalised to unity. Note that, in the case of the lepton and light quark jet, the curves coincide.

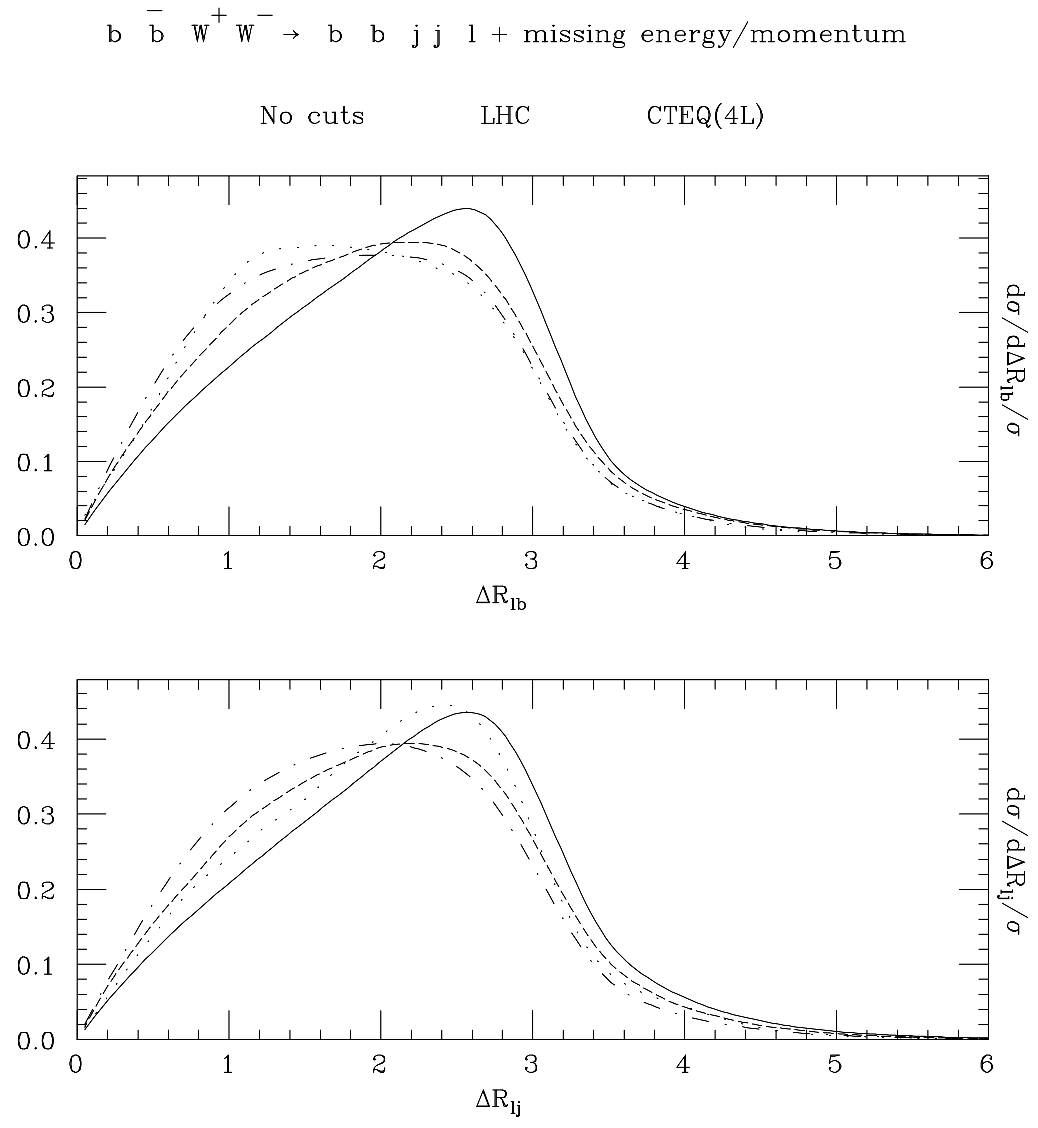

Figure 4: Differential spectra in pseudorapidity-azimuth separation between the following pairs of particles in $W^\pm H^\mp$ and $t\bar{t}$ events: lepton/b jet (top); lepton/light quark jet (bottom). Here, $\tan\beta = 30$ and the $W^\pm H^\mp$ rates are plotted for $M_{H^\pm} = 214$ (solid), 407 (dashed) and 605 (dotted) GeV. As $M_{H^\pm} > m_t + m_b$, $t\bar{t}$ events have no MSSM parameter dependence (dot-dashed). No cuts have been implemented. The PDFs CTEQ(4L) have been used. Distributions are normalised to unity.

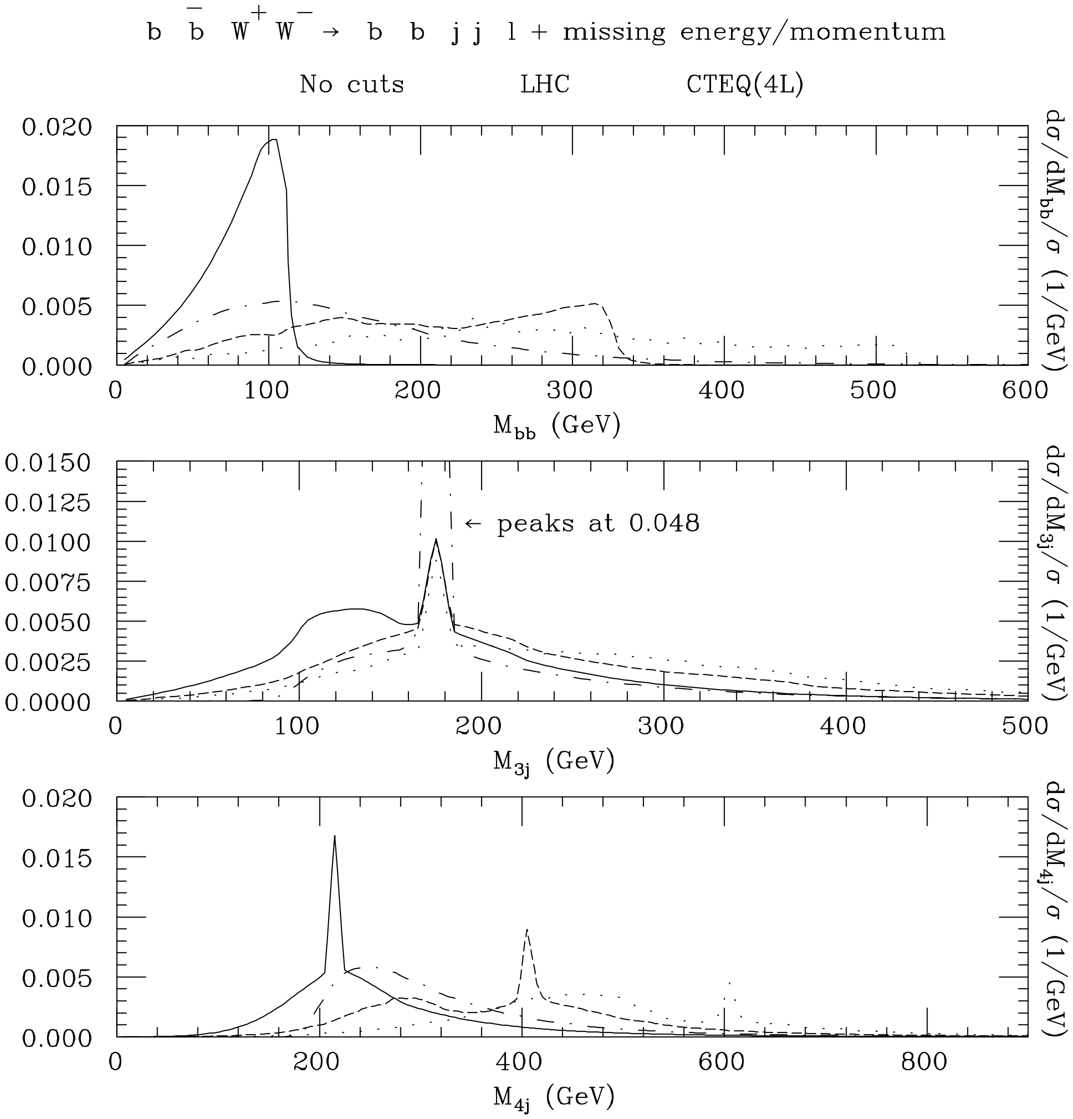

Figure 5: Differential spectra in invariant mass for the following systems in $W^\pm H^\mp$ and $t\bar{t}$ events: bb (top); three jet (middle); four jet (bottom). Here, $\tan\beta = 30$ and the $W^\pm H^\mp$ rates are plotted for $M_{H^\pm} = 214$ (solid), 407 (dashed) and 605 (dotted) GeV. As $M_{H^\pm} > m_t + m_b$, $t\bar{t}$ events have no MSSM parameter dependence (dot-dashed). No cuts have been implemented. The PDFs CTEQ(4L) have been used. Distributions are normalised to unity.

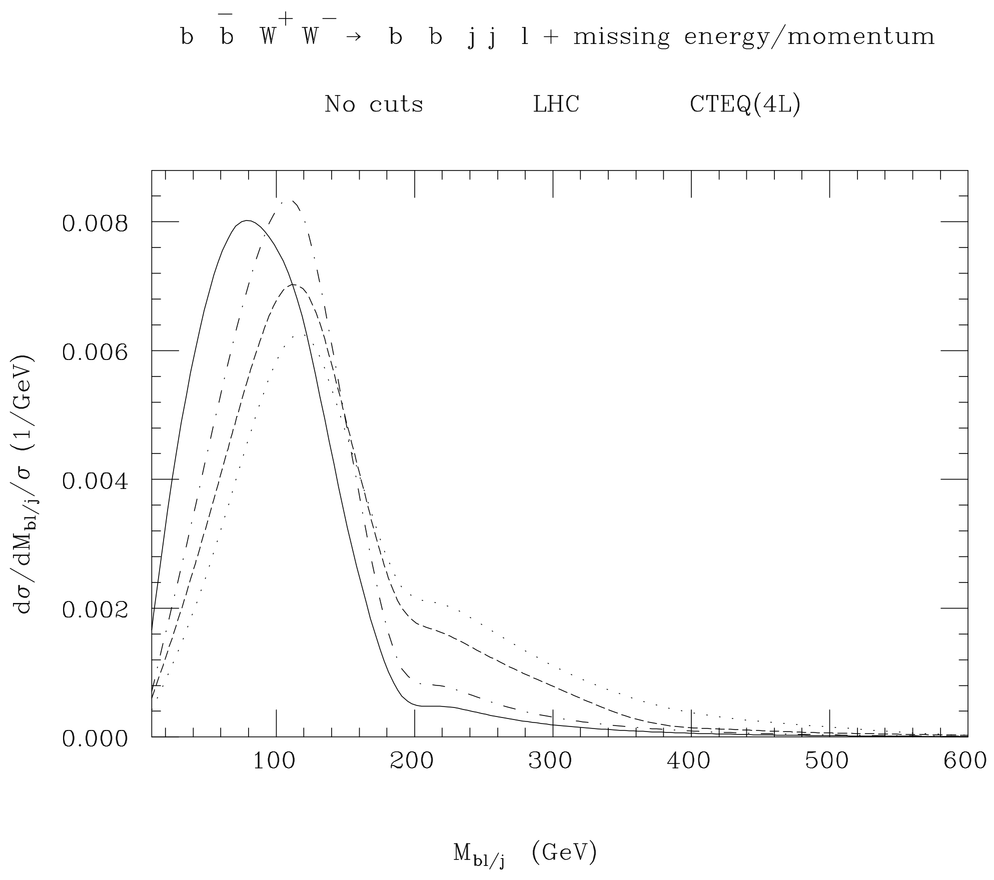

Figure 6: Differential spectra in invariant mass for the $b\ell$/jet system in $W^\pm H^\mp$ and $t\bar{t}$ events. Here, $\tan\beta = 30$ and the $W^\pm H^\mp$ rates are plotted for $M_{H^\pm} = 214$ (solid), 407 (dashed) and 605 (dotted) GeV. As $M_{H^\pm} > m_t + m_b$, $t\bar{t}$ events have no MSSM parameter dependence (dot-dashed). No cuts have been implemented. The PDFs CTEQ(4L) have been used. Distributions are normalised to unity.

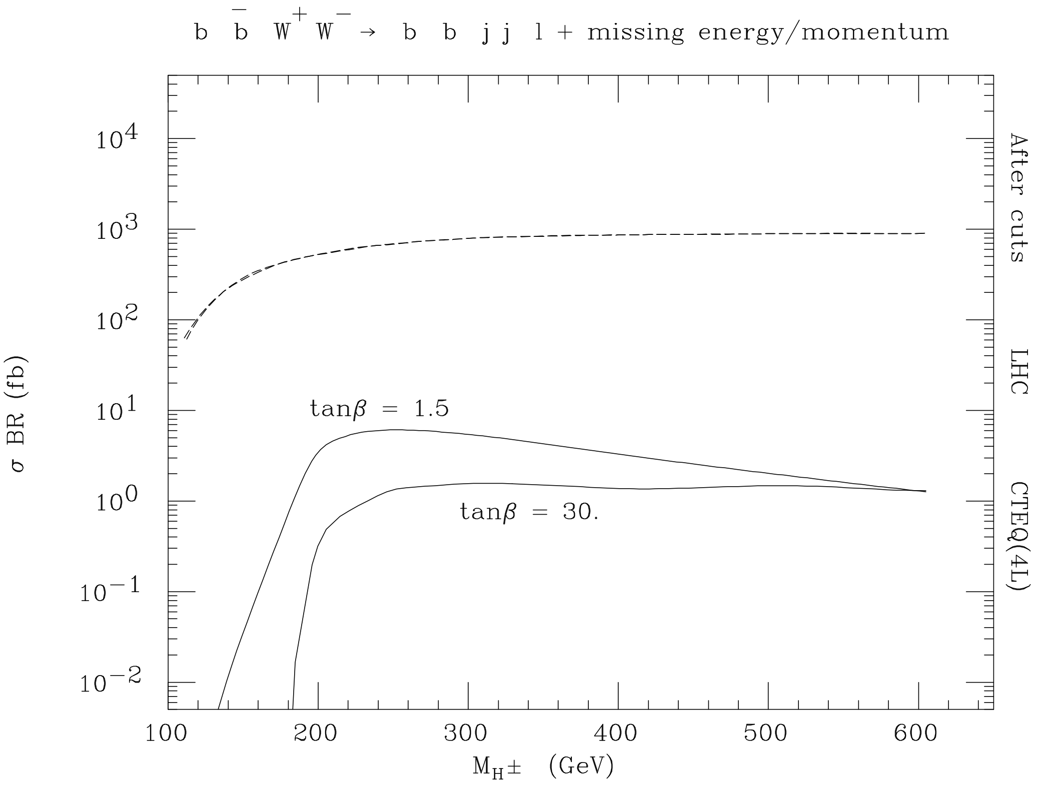

Figure 7: Total event rates for $W^{\pm}H^{\mp}$ (solid) and $t\bar{t}$ production (dashed) at the LHC, after the selection cuts have been implemented, using CTEQ(4L), as a function of $M_{H^{\pm}}$ for $\tan\beta = 1.5$ and $\tan\beta = 30$.

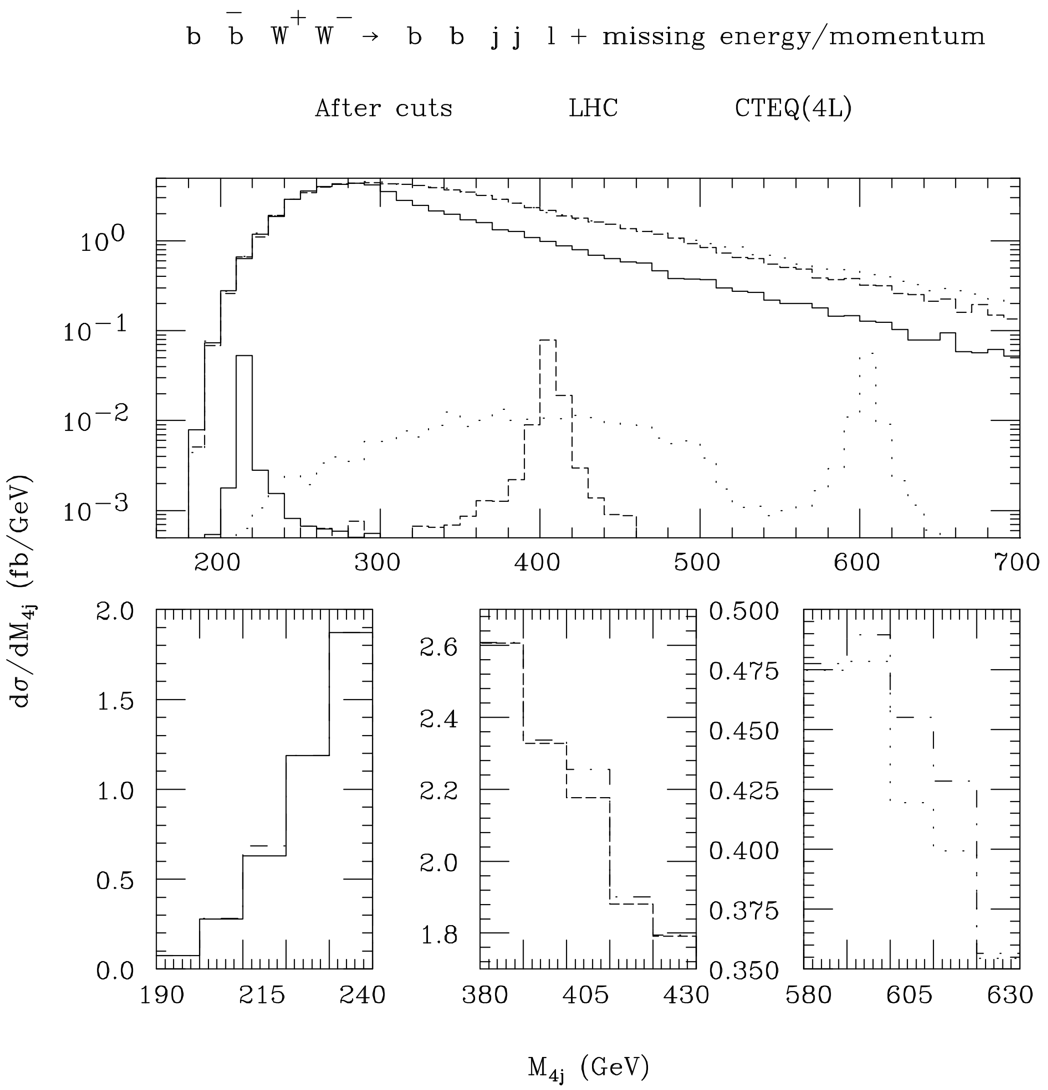

Figure 8: Differential spectra in the four jet invariant mass in $W^{\pm}H^{\mp}$ and $t\bar{t}$ events for $\tan\beta = 30$ and $M_{H^{\pm}} = 214$ (solid), 407 (dashed) and 605 (dotted) GeV. Their sum (dot-dashed) is also reported in the three blow up frames below, compared against the $t\bar{t}$ rates from above. Even though $M_{H^{\pm}} > m_t + m_b$, $t\bar{t}$ events have a MSSM parameter dependence due to an $M_{H^{\pm}}$ based constraint being implemented in the selection cuts. The PDFs CTEQ(4L) have been used. Distributions are normalised to total cross sections.